Ulysses Observations of the Magnetic Connectivity between CMEs and the Sun

Pete Riley

Science Applications International Corporation, San Diego, CA 92121

J .T. Gosling

Los Alamos National Laboratory, MS D466, Los Alamos, NM 87545

N. U. Crooker

Center for Space Physics, Boston University, 725 Commonwealth Ave., Boston, MA 02215

ABSTRACT

We have investigated the magnetic connectivity of coronal mass ejections (CMEs) to the Sun using Ulysses observations of suprathermal electrons at various distances between 1 AU and 5.2 AU. Drawing on ideas concerning the eruption and evolution of CMEs, we had anticipated that there might be a tendency for CMEs to contain progressively more open field lines, as reconnection back at the Sun either opened or completely disconnected previously closed field lines threading the CMEs. Our results, however, did not yield any discernible trend. By combining the potential contribution of CMEs to the heliospheric flux with the observed build-up of flux during the course of the solar cycle we also derive a lower limit for the reconnection rate of CMEs that is sufficient to avoid the "flux catastrophe" paradox. This rate is well below our threshold of detectibility.

Subject headings: Sun: coronal mass ejections (CMEs)– Sun: activity–Sun: corona–Sun: magnetic fields–solar wind

1. Introduction

In this paper, we analyze the connectivity of magnetic field lines within Coronal Mass Ejections (CMEs) observed by Ulysses during its in-ecliptic passage to Jupiter using observations of suprathermal electrons (Phillips 1997). Typically in the ambient solar wind, there exists a single beam of suprathermal electrons flowing along field lines away from the Sun. Sometimes two antiparallel beams are observed. Although the anti-parallel beams can in

principle be caused by a number of processes (Gosling et al. 2001), these counterstreaming suprathermal electrons (CSEs) are often the result of the field lines being rooted at the Sun at both ends. Thus measurements of suprathermal electrons provide a unique opportunity to study the connectivity of field lines within CMEs.

Early observations of CMEs by Skylab suggested that the foot-points of CMEs remained connected to the solar surface. This, however, led to the apparent paradox that the magnetic flux in the heliosphere would build up without limit (e.g., Gosling (1975); McComas et al. (1992)), which is clearly not observed. Gosling et al. (1995a), drawing on similarities between the evolution of the magnetic field in the Earth's magnetotail and CME eruptions, proposed a picture of three-dimensional reconnection within the magnetic legs of CMEs that would minimize heliospheric flux build-up. They suggested that closed field lines threading an CME reconnect with other closed field lines and with nearby open field lines to reduce the net flux added to the heliosphere.

Within the context of the magnetic connectivity of CMEs to the Sun, it is important to clarify what types of reconnection we believe to be occurring and which one(s) play a role in moderating the build-up of heliospheric flux. Gosling et al. (1995b) and Crooker et al. (2002a) have identified 4 basic modes of reconnection that have the potential to reduce the magnetic flux in the heliosphere: (1) reconnection between two open field lines; (2) reconnection of a closed field line with itself; (3) reconnection of a closed field line with another closed field line; and (4) reconnection of a closed field line with an open field line. Reconnection of type 2 leads to the formation of closed plasmoids and is likely an artifact of an idealized 2-D geometry. Type 3 reconnection is the 3-D generalization of type 2, and provides a natural explanation of the development of a flux rope within a CME, while simultaneously ensuring that both ends of the flux rope remain rooted to the Sun. Finally, type 4 reconnection has been invoked to describe a process of field line transport on the Sun (Wang & Sheeley 1993; Schrijver et al. 1998; Fisk et al. 1999), a possible source for the slow solar wind (Wang et al. 1998), and as a way to limit the flux build-up without disconnection (Gosling et al. 1995a; Crooker et al. 2002a).

In this study we are concerned primarily with type 3 (partial disconnection) and type 4 (interchange reconnection). Partial disconnection does substantially reduce the amount of flux that would otherwise be injected into the heliosphere, yet it does not open any field lines within a CME. Interchange reconnection, on the other hand, provides a natural way of eroding closed field lines within CMEs. In particular, it is the only mode of reconnection we are aware of that is capable of producing open field lines intermingled with closed ones. One of the predicted signatures of interchange reconnection is the presence of magnetic field inversions, where the strahl is predominantly parallel (antiparallel) to the field, indicating

away (toward) magnetic polarity, yet the locally measured field points toward (away from) the Sun (Crooker et al. 1998b,a).

Shodhan et al. (2000) analyzed the relationship between CSEs and magnetic cloud (MC) signatures for 34 MCs observed at 1 AU in the ecliptic plane. The events were distributed over different phases of the solar cycle. They found that the percentage of a MC containing CSE intervals ranged from 0% to 100%. On average, CSE intervals spanned 59% of the MCs. The clouds with no CSEs all occurred at solar minimum, whereas less than half of the events with 100% CSEs occurred at solar minimum. While the CSE intervals were distributed randomly throughout the MCs, there was a linear dependence of the percentage of closed field lines within a MC on the size of the cloud: Larger clouds tended to have proportionately more counterstreaming. Crooker et al. (2002b) extended the work of Shodhan et al. (2000) by analyzing 31 MCs observed by Ulysses at 5 AU in the ecliptic plane. They found similar results: the MCs at 5 AU were 45% open (i.e., CSE intervals spanned 55% of the MCs, on average) as compared to 41% at 1 AU; and larger clouds tended to be more closed than smaller clouds.

The present work differs from these previous studies in several respects. Here we analyze the set of CMEs observed by Ulysses during its in-ecliptic passage to Jupiter. The events all fall within a roughly 1 year time span and any effects related to solar cycle variations are minimized. In addition, we do not distinguish between CMEs and MCs: We adopt the view that MCs represent a readily distinguishable subset of CMEs.

The remainder of this paper is structured as follows. First, we estimate a lower limit to the reconnection rate that is required to avoid the "flux catastrophe" paradox. Next we summarize the selection procedure for the events used in this study. After describing one event in detail, we then discuss the statistical properties of all the events. Finally, we summarize the main results of the study and discuss their implications.

2. An estimate of the Lower Limit of the Reconnection Rate

As discussed in Section 1, CMEs propagating away from the Sun typically carry field lines rooted at the Sun at both ends. As such, they introduce new magnetic flux into the heliosphere that was not part of the ambient solar wind expansion. This has led to the so-called "flux catastrophe" paradox (e.g., McComas et al. (1992)). In particular, if CMEs add new flux, why doesn't the IMF magnitude grow without limit? Reconnection, which can close newly opened field lines, can reduce the flux and avoid the "catastrophe". Drawing on the results of McComas et al. (1992) we can estimate how fast this reconnection must proceed.

Calculating a pseudo-flux based on in-ecliptic in situ measurements of the IMF McComas et al. found that: (1) In the absence of other processes, the contribution of flux from CMEs would cause the heliospheric flux in the eclipic plane to double in 9 months; and (2) this same pseudo-flux varied only by a factor of 2 between solar minimum and solar maximum. To obtain an order of magnitude estimate of the reconnection rate from these results, we can ask what average percentage of CME field lines could be closed at the edge of the heliosphere (say at 50 AU for simplicity) to be consistent with (1) and (2)? If we assume an CME at 1 AU has %CSE=100, then by 50 AU this must drop to $100\% \times \frac{9}{66} = 13.46\%$, where the time interval of 66 months (5.5 years) represents the interval between solar minimum and maximum. Expressed as a rate, this would be 1.76%/AU.

3. Selection of Events

The CMEs encountered by Ulysses during its outward passage to Jupiter were identified primarily by the presence of counterstreaming suprathermal electrons (CSEs). In addition, it was required that at least one other characteristic commonly associated with ejecta (e.g., anomalously low proton temperature, high helium abundance, rotation of the magnetic field, etc) also be present (Phillips 1997). These combined criteria led to the identification of 25 CMEs. Among these events there was, however, considerable variability. Many, for example, did not display helium abundance enhancements or rotations in the magnetic field, which are commonly associated with flux ropes. And in some cases the boundaries of the ejecta were difficult to ascertain.

To mimimize variability due to "glancing" trajectories through an CME, we further restricted our analysis to only those events for which at least two other plasma and/or magnetic field signatures were present in addition to the signature of CSEs. By so doing, our initial list of 25 events was reduced to 17.

4. Case Study

To illustrate some of the main features of these events, we have chosen the May 29-31, 1991 CME, which also happened to be a magnetic cloud (or flux rope). Figure 1 summarizes the main plasma and magnetic measurements for a period of 10 days encompassing the event. The CME interval is marked by the 2 vertical lines. As with all of the events, this CME was initially identified based on the presence of CSEs, which appear as intense (red) fluxes parallel and anti-parallel to the magnetic field (i.e., 0^o and 180^o pitch angles). In addition,

this event showed depressed density ($< 0.1cm^{-3}$), temperature ($< 4 \times 10^4 K$), and plasma beta (< 0.01). The speed profile monotonically decreased indicating that the ejecta was expanding (since the leading edge was traveling away from the Sun faster than the trailing edge). Within the ejecta, the ratio of alpha particles to protons was elevated and variable. The magnetic field magnitude, on the other hand, while slightly elevated, remained flat with little variance. The magnetic field angles showed monotonic changes, with the dominant rotation in the meridional plane. This is consistent with the flux rope axis lying primarily in the ecliptic plane, perpendicular to the radial direction.

The boundaries of the CME were deduced by a visual inspection of variations in all parameters. For this particular event, discontinuous changes in the alpha particle to proton ratio coupled with the field rotations and the presence of CSEs established the boundaries marked in Figure 3. We estimated the time occupied by CSEs for this CME to be 1.789 days. The duration of the CME was 2.477 days, and thus the percentage of the CME containing closed magnetic fields was 72%. These boundaries are, however, not definitive and this example was chosen in part to illustrate some of the complexities in identifying CME boundaries. Using the CSEs and the helium/proton ratio signatures as primary signatures, for example, one might be tempted to move the leading edge earlier in time by ~ 0.5 day. It is also worth noting that the termination of the CSE signature is not obviously associated with any changes in the other parameters. In view of the disparity between the CSE signature and the other magnetofluid parameters, a lack of correlation between them is not unexpected.

5. Statistical Properties of the Events

Using the procedure described above, we identified the boundaries of all 17 CMEs as well as intervals of CSEs and Heat Flux Dropouts (HFDs, i.e., intervals without suprathermals in either direction). The results are summarized in Table 1. Only one event contained any identifiable HFDs. The average value of the percentage of the CME occupied by CSES (%CSE) was 69%, but ranged from 34% to 100%. Figure 2a displays the variation of %CSE with increasing heliocentric distance. A least-squares fit line has been drawn through the points with a slope of 0.2%/AU, yet there is no clearly observable trend in %CSE with increasing distance from the Sun. In Figure 2b we have overlaid a set of of lines representative of the lower limit to the reconnection rate derived in Section 2. Clearly such a modest trend is below our threshold of detectibility. Since it could be argued that the rate of reconnection is more likely to be a function of time rather than distance, we have recast the results as a function of "age" of the CME in the solar wind, where age is defined as the distance of the CME from the Sun divided by its average speed. These results are shown in Figure 2c. The

slope of the least-squares fit line is 0.3%/day. In absolute terms, a 2% drop in Figure 2a in going from 1 to 5.4 AU has increased to 6% in Figure 2c. While this trend is suggestive, the large scatter in the data precludes us from making any firm conclusions about trends with either distance or "age" of the CMEs.

6. Summary and Discussion

In this study we have analyzed the streaming properties of suprathermal electrons for 17 CMEs observed by Ulysses during its outward-bound trip to Jupiter. Our results did not yield a detectable trend in the %CSEs within CMEs with increasing heliocentric distance (or time). If such an underlying trend really does exist, then it must be below the threshold that can be measured employing the techniques outlined here. We also derived a lower limit to the reconnection rate based on arguments avoiding the "flux catastrophe" paradox. This rate would be statistically undetectable within the scatter of our results.

Ideally we would like to sample the same CME as it propagates away from the Sun. To a limited extent, this was achieved by Skoug et al. (2000) who identified a magnetic cloud that was observed by both ACE at 1 AU and Ulysses at 5.4 AU. At the time the spacecraft were nearly radially aligned with a latitudinal separation of $\sim 2.2^o$ and a longitudinal separation of $\sim 5.5^o$. At Ulysses $\sim$ 71% of the cloud contained CSEs whereas at ACE only limited intervals of CSEs were observed within the cloud. Moreover, these intervals were possibly shock-associated and thus not indicative of the presence of closed field lines. Thus we infer that the CME observed at Ulysses contained significantly more closed field lines than the event at ACE. This runs counter to our expectation that field lines embedded within CMEs open up as the ejecta propagates away from the Sun, suggesting that the degree to which closed field lines are observed is quite sensitive to the spacecraft's trajectory through the event. By extension, the variability we have seen in the Ulysses in-ecliptic CMEs may well represent spatial variations that are present in every event, as well as intrinsic differences between the events.

One of the largest potential uncertainties comes from the determination of the CME boundaries and its impact is also the most difficult to assess. Boundary identification is as much of an art as a science. We can reduce errors by retaining only those events in which we have sufficient confidence, but even the quintessential cases are not beyond question. Consider the case study described in section 3 and shown in Figure 1. Given the subsequent appearance of CSEs following the event, it could be argued that the trailing boundary occurred 3 days beyond its current placement. By so doing, the new structure would: (1) span a sector boundary; (2) include a characteristic quasi-symmetric return of the meridional

angle of the magnetic field vector, θ_B, from high elevations; and (3) be nearly completely filled with CSEs. Indeed these characteristics fit well with the pattern described by Crooker et al. (1998b) where it was inferred that the spacecraft passed through both legs of a flux rope loop (although we should note that Kahler et al. (1999) have disputed this interpretation). Instead, we believe that the CSEs occurring after the trailing boundary shown in Figure 1 were generated at the shock that occurred late on day 154 (not shown). The main point to be drawn from this discussion is that boundary identification is often difficult and so should be viewed with an appropriate degree of caution. Moreover, these boundaries are not independent of the picture or model one has for the structure of CMEs. For example, compositional changes often identify solar material of a different origin than that of the surrounding solar wind. Likewise, coherent structures in the magnetic field can indicate the presence of a single large-scale structure. If the two do not match up, however, to which do we assign the greater weight? Ultimately, we may conclude that there exist multiple fundamental boundaries associated with an individual event. Understanding what each boundary signifies, and what the relationship is between them, may lead us to a deeper insight into CMEs and their mechanism(s) of eruption.

Our procedure for initially identifying and defining CME boundaries relied in part on the presence of CSEs. While we are not aware of any events that were overlooked using this approach, we note that Shodhan et al. (2000), Crooker et al. (2002b), and Gosling & Forsyth (2001) found cases with 0% CSEs. Their selection criteria was purposely chosen to be independent of CSE signatures. While this bias has no obvious impact on the results and conclusions of this study, it may account for the slightly higher %CSEs that were obtained in this study.

In closing, we note that one of the predictions of interchange reconnection is the production of magnetic field inversions. Figure 1, for example, clearly shows that the open field in the CME is inverted: The dominant strahl is parallel to the field, indicating "away" polarity, while the local field points toward the Sun ($\phi_B \sim +90^o$). This suggests that an important topic for future study is to assess quantitatively to what extent these inversions are present on open field lines in CMEs. We suggest that on average, it should occur 50% of the time, depending upon which segment of the inversion the spacecraft intercepts.

PR gratefully acknowledges the support of the National Aeronautics and Space Administration (LWS Program) and the National Science Foundation (SHINE Program and the Center for Integrated Space Weather Modeling) in undertaking this study. NUC would like to acknowledge support from NASA (NAG5-10881). Work by JTG was supported by Ulysses project funds.

REFERENCES

Balogh, A., Beek, T. J., Forsyth, R. J., Hedgecock, P. C., Marquedant, R. J., Smith, E. J., Southwood, D. J., & Tsurutani, B. T. 1992, Astron. Astrophys. Suppl. Ser., 92, 221

Bame, S. J., McComas, D. J., Barraclough, B. L., Phillips, J. L., Sofaly, K. J., Chavez, J. C., Goldstein, B. E., & Sakurai, R. K. 1992, Astron. Astrophys. Suppl. Ser., 92, 237

Crooker, N. U., Gosling, J. T., & Kahler, S. W. 1998a, J. Geophys. Res., 103, 301

—. 2002a, J. Geophys. Res. (Space Physics), 107(2), abstract SSH 3

Crooker, N. U., Gosling, J. T., Kahler, S. W., Forsyth, R. J., & Rees, A. 2002b, in American Geophysical Union, Fall Meeting 2002 (San Francisco, CA: AGU), abstract SH21A

Crooker, N. U., McAllister, A. H., Fitzenreiter, R. J., Linker, J. A., Larson, D. E., Lepping, R. P., Szabo, A., Steinberg, J. T., Lazarus, A. J., Mikić, Z., & Lin, R. P. 1998b, J. Geophys. Res., 103, 26859

Fisk, L. A., Zurbuchen, T. H., & Schwadron, N. A. 1999, Astrophys. J., 521, 868

Gosling, J. T. 1975, Reviews of Geophysics and Space Physics, 13, 1053

Gosling, J. T., Bame, S. J., Feldman, W. C., McComas, D. J., Phillips, J. L., & Goldstein, B. E. 1993, Geophys. Res. Lett., 20, 2335

Gosling, J. T., Birn, J., & Hesse, M. 1995a, Geophys. Res. Lett., 22, 869

Gosling, J. T., & Forsyth, R. J. 2001, Space Science Reviews, 97, 87

Gosling, J. T., McComas, D. J., Phillips, J. L., Pizzo, V. J., Goldstein, B. E., Forsyth, R. J., & Lepping, R. P. 1995b, Geophys. Res. Lett., 22, 1753

Gosling, J. T., Skoug, R., & Feldman, W. C. 2001, Geophys. Res. Lett., 28, 4155

Kahler, S. W., Crooker, N. U., & Gosling, J. T. 1999, J. Geophys. Res., 104, 9911

McComas, D. J., Gosling, J. T., & Phillips, J. L. 1992, J. Geophys. Res., 97, 171

Moldwin, M. B., Scime, E. E., Bame, S. J., Gosling, J. T., Phillips, J. L., & Balogh, A. 1993, Planet. Space Sci., 41, 795

Phillips, J. L. 1997, in Rep. 97-1086, Los Alamos Natl. Lab., Los Alamos, N.M.

Schrijver, C. J., Title, A., Harvey, K. L., Sheeley, Jr., N. R., Wang, Y. M., van den Oords, G. H. J., Shine, R. A., Tarbell, T. D., & Hurlburt, N. E. 1998, Nature, 394, 152

Shodhan, S., Crooker, N. U., Kahler, S. W., Fitzenreiter, R. J., Larson, D. E., Lepping, R. P., Siscoe, G. L., & Gosling, J. T. 2000, J. Geophys. Res., 105, 27261

Skoug, R. M., Feldman, W. C., Gosling, J. T., & McComas, D. J. 2000, J. Geophys. Res., 105, 23069

Wang, Y. M., & Sheeley, Jr., N. R. 1993, Astrophys. J., 414, 916

Wang, Y. M., Sheeley, Jr., N. R., Walters, J. H., Brueckner, G. E., Howard, R. A., Michels, D. J., Lamy, P. L., Schwenn, R., & Simnett, G. M. 1998, Astrophys. J., 498, L165

Fig. 1.— Plasma and magnetic measurements encompassing May 29-31, 1991 CME. From top to bottom: Color-coded pitch angle distributions for electrons in the energy range 84-115 eV, proton number density, proton temperature, bulk solar wind speed, the alpha to proton ratio, the magnetic field magnitude, the azimuthal and meridional angles of the magnetic field, and the plasma beta. The pitch angle distributions are plotted in the spacecraft frame. For these energies and at this epoch, differences between the spacecraft frame and solar wind frame are small.

Fig. 2.— Percentage of CME occupied by counterstreaming as a function of: (a) heliocentric distance; (b) also heliocentric distance, where the dashed lines are a sequence of straight lines with slope -1.55%/AU; and (c) time.

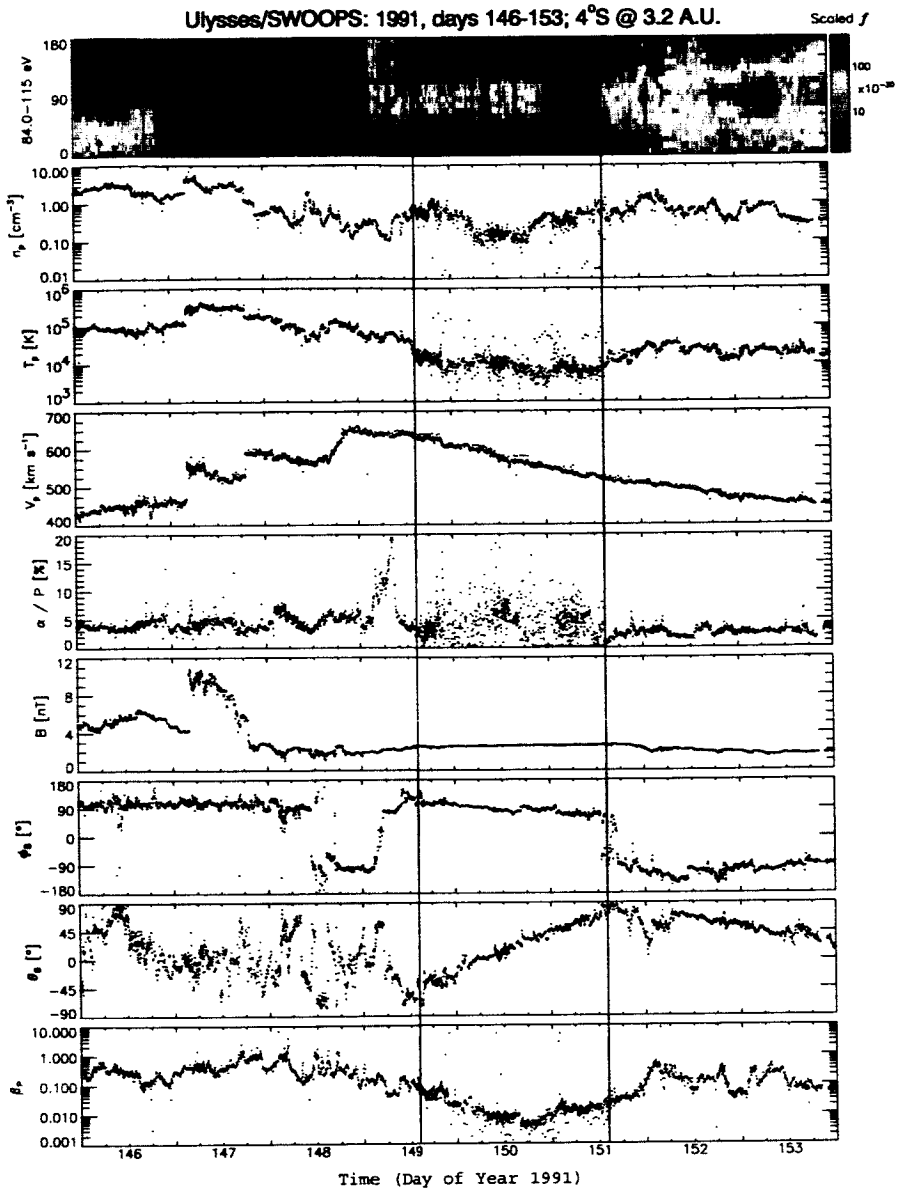
Ulysses/SWOOPS: 1991, days 146-153; 4°S @ 3.2 A.U.
Scaled f
84.0–115 eV
180
90
0
100
x10⁻³⁰
10
n_p [cm^{-3}]
10.00
1.00
0.10
0.01
T_p [K]
10^6
10^5
10^4
10^3
V_p [km s^{-1}]
700
600
500
400
α / P [%]
20
15
10
5
0
B [nT]
12
8
4
0
ϕ_B [°]
180
90
0
−90
−180
θ_B [°]
90
45
0
−45
−90
β_p
10.000
1.000
0.100
0.010
0.001
146
147
148
149
150
151
152
153
Time (Day of Year 1991)

Figure 1

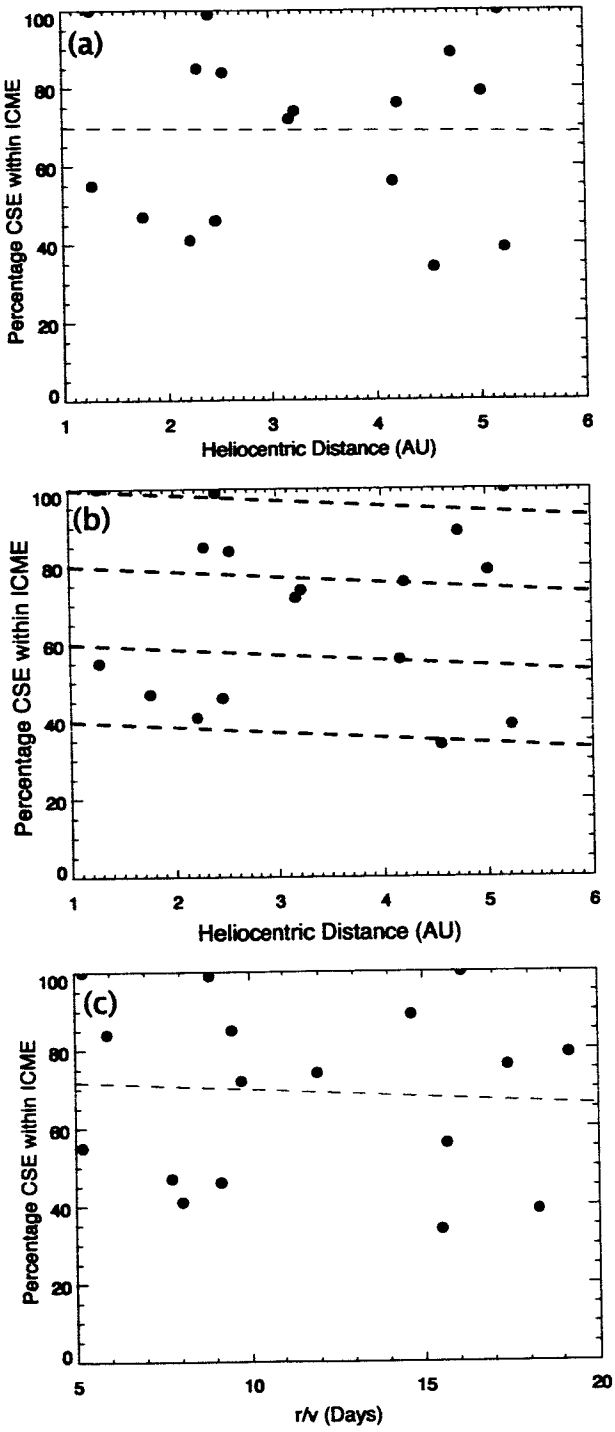
(a)
Percentage CSE within ICME
Heliocentric Distance (AU)
(b)
Percentage CSE within ICME
Heliocentric Distance (AU)
(c)
Percentage CSE within ICME
r/v (Days)

Figure 2

Table 1: Magnetic Connectivity Properties of Coronal Mass Ejections used in this Study

Start Date	CSE (days)	HFD (days)	Total Time (days)	% CSE	% HFD	r
11/29/90	0.141	0.000	0.141	100	0	1.28
12/01/90	0.188	0.000	0.336	55	0	1.28
01/16/91	1.234	0.000	2.625	47	0	1.77
02/27/91	0.312	0.000	0.758	41	0	2.21
03/05/91	2.523	0.000	2.953	85	0	2.29
03/15/91	2.578	0.000	2.594	99	0	2.41
03/21/91	0.273	0.000	0.586	46	0	2.46
03/27/91	1.781	0.000	2.117	84	0	2.53
05/29/91	1.789	0.000	2.477	72	0	3.18
06/04/91	2.000	0.000	2.695	74	0	3.23
09/10/91	1.719	0.539	3.023	56	17	4.17
09/18/91	0.766	0.000	1.000	76	0	4.22
10/27/91	0.422	0.000	1.227	34	0	4.55
11/17/91	2.984	0.000	3.352	89	0	4.73
12/27/91	0.633	0.000	0.797	79	0	5.02
01/12/92	1.180	0.000	1.180	100	0	5.18
01/21/92	0.367	0.000	0.938	39	0	5.22

8. Appendix 4

Kinematic treatment of CME evolution in the solar wind

Pete Riley, and N. U. Crooker

In press, *Astrophysical Journal,* 2004.